LAMINAR FREE CONVECTION HEAT TRANSFER

FROM VERTICAL CYLINDERS

A THESIS

Presented to

the Faculty of the Graduate Division

by

Joe Bradley Cox

In Partial Fulfillment

of the Requirements of the Degree

Master of Science in Mechanical Engineering

Georgia Institute of Technology

September, 1962

5 S
12 R

LAMINAR FREE CONVECTION HEAT TRANSFER FROM VERTICAL CYLINDERS

Approved:

Date approved by Chairman: Sept. 10, 1962

ACKNOWLEDGMENTS

I wish to thank my advisor, Dr. Charles W. Gorton who suggested this topic, for his advice and encouragement. I appreciate the comments of Professor K. R. Purdy and Dr. J. D. Fleming who read this thesis.

I would also like to express my appreciation to my parents who have always been a source of encouragement.

TABLE OF CONTENTS

LIST OF TABLES

LIST OF FIGURES

SUMMARY

The problem considered was laminar free convection heat transfer from a vertical isothermal circular cylinder for the case where the effect of curvature was important.

Average heat transfer coefficients were determined experimentally for laminar free convection heat transfer from a vertical electrically heated wire. Tests were run in three fluids: water, mineral oil, and air. The wire was platinum, 0.01594 in. in diameter and 2.59 in. long. It was heated by current from a twelve volt storage battery. Measurements were made of the power input, ambient fluid temperature and wire temperature. The wire was calibrated as a resistance thermometer so that its temperature could be determined from a resistance measurement. This resulted in an average value of the wire temperature.

Higher average heat transfer coefficients were obtained for the wire than would have been possible with a flat plate subjected to the same boundary conditions. The influence of curvature was less significant for the fluids with the higher Prandtl numbers.

The experimental results compared well with the analytical solutions of Hama, Recesso, and Christiaens (5) and Le Fevre and Ede (4).

The results were presented in both tabular and graphical forms which gave the ratio of the average Nusselt numbers for the cylinder and flat plate as a function of ξ, where

$$\xi = \frac{2^{\frac{3}{2}}}{Gr_L^{\frac{1}{4}}} \frac{L}{r_o} .$$

ξ ranged from 7.72 to 20.2 for water, 25.0 to 66.2 for oil, and 24.0 to 34.1 for air. The Grashof number based on the wire length ranged from 4.11×10^6 to 2.01×10^8 for water, 3.71×10^4 to 1.84×10^6 for oil, and 5.29×10^5 to 2.15×10^6 for air.

CHAPTER I

INTRODUCTION

The problem investigated in this research was laminar free convection heat transfer from a vertical wire. Heat transfer by free convection occurs whenever an object at some arbitrary temperature is allowed to contact a fluid at a different temperature. The fluid near the surface of the object experiences a change in density due to the temperature difference which exists between the body and the surrounding fluid. The fluid adjacent to the surface will move either up or down, depending upon whether it is heated or cooled by the surface, and in this manner currents are established in a region near the body. This motion takes place in a relatively thin layer of fluid called the hydrodynamic boundary layer. The region near the surface where the fluid temperature is significantly different from the ambient temperature is known as the thermal boundary layer. It is the convection current, transporting heated or cooled fluid away from the body, that effects the phenomenon of free convection heat transfer. Generally, and this is the case in the present research, the force causing the motion of the fluid is due to the earth's gravity. In the analysis of free convection problems, it makes no difference whether the fluid is heated or cooled by the immersed body, because the non-dimensionalized differential equations which describe the heat transfer process are identical for the two cases.

Laminar free convection heat transfer from vertical circular cylinders and vertical flat plates are related. Merk and Prins (1)* have shown that for identical boundary conditions and equal distances from the leading edge, the local laminar free convection heat transfer coefficients are the same for the vertical isothermal flat plate and the vertical isothermal circular cylinder when the radius of the cylinder is much larger than its boundary layer thickness. Ostrach (2) solved the laminar free convection boundary layer equations for the vertical isothermal flat plate for several Prandtl numbers using a digital computer.

Sparrow and Gregg (3) solved the laminar free convection boundary layer equations for the case of the vertical isothermal cylinder for Prandtl numbers of 0.72 and 1.0 by using a series solution. They began with abbreviated forms of the Navier-Stokes equations, energy equation, and continuity equation which were obtained after an order analysis, and assumed steady state conditions and constant fluid properties with the exception of the density. Viscous dissipation and work against the gravity field were neglected. Solutions were obtained numerically with a digital computer for Prandtl numbers of 0.72 and 1.0. The Sparrow and Gregg solution was of the form

$$\frac{Nu_{L\ cyl}}{Nu_{L\ fp}} = f(\xi,\ Pr)$$

where ξ was defined as

$$\xi \equiv \frac{2^{\frac{3}{2}}}{Gr_L^{\frac{1}{4}}}\ \frac{L}{r_o}\ .$$

*Numbers in parentheses refer to references in the Bibliography.

(A complete list of symbol definitions is given in the Nomenclature in Appendix D, p. 48.) Curves were plotted for the solution in the range of ξ from 0 to 1.

LeFevre and Ede (4) used the integral boundary layer relations and a series approximation to obtain an approximate solution for laminar free convection from a vertical isothermal circular cylinder. Their solution was

$$\frac{Nu_{L\ cyl}}{(Gr_L Pr)^{\frac{1}{4}}} = \frac{4}{3}\left[\frac{7\ Pr}{5(20 + 21\ Pr)}\right]^{\frac{1}{4}} + \frac{4}{35}\left[\frac{272 + 315\ Pr}{64 + 63\ Pr}\right]\left[\frac{D}{L}(Gr_L Pr)^{\frac{1}{4}}\right]^{-1}$$

This solution is shown in Figures 7, 8, and 9 beginning on p. 22, for Prandtl numbers of 0.72, 4.52, and 162.

Among the more recent investigators of the problem of laminar free convection from a vertical circular cylinder with uniform wall temperature, Hama, Recesso, and Christiaens (5) solved the integrated boundary layer equations, simplified considerably by discarding the inertia term in the momentum equation. Their solution is

$$\left(\frac{1}{8}\right)e^{4\alpha} - \left(\frac{\alpha}{9}\right)e^{3\alpha} + \left(\frac{1}{9}\right)e^{3\alpha} - \frac{e^{4\alpha}-1}{4\alpha} + \frac{e^{2\alpha}-1}{2\alpha} + \tag{1}$$

$$\frac{3}{8}\int_0^{4\alpha}\frac{e^t-1}{t}\,dt - \frac{2}{27}\int_0^{3\alpha}\frac{e^t-1}{t}\,dt - \frac{1}{2}\int_0^{2\alpha}\frac{e^t-1}{t}\,dt -$$

$$\frac{17}{27} = \frac{1}{Pr}\ \frac{2\nu^2}{g\beta(t_w-t_\infty)r_o^3}\ \frac{X}{r_o} = \frac{1}{32Pr}\ \xi^4$$

This solution was not quite accurate for small values of ξ because the assumed profiles were slightly in error for small ξ. They recommended that the values of ξ obtained by the above equation be reduced by 8.5 per cent for a Prandtl number of 0.72 in order to obtain agreement with the flat plate solution, i.e., $\xi = 0$. Their recommended values compared well with data they obtained from tests conducted on vertical isothermal cylinders in air in the range of ξ from 3.1 to 56, and with the Sparrow and Gregg solution for $\xi \leq 1.0$ and $Pr = 0.72$. Recommended values of $1/\alpha$, the dimensionless local heat transfer coefficient, versus ξ were tabulated in the range of ξ from 0.107 to 43.1 in Reference (5).

CHAPTER II

INSTRUMENTATION AND EQUIPMENT

One of the major problems encountered in planning this experiment was that of measuring the temperature of the test wire. Most of the work that has been accomplished on free convection from vertical cylinders has been done with cylinders with diameters large enough to allow thermocouples to be run radially outward from the hollow inside to the outside surface. This technique eliminated the problem of thermocouples or other temperature measuring probes disturbing the free convection boundary layer by protruding from the cylinder surface. Because of the small diameter of the wire used in the present test, it would have been impossible to run thermocouples through the wire, and temperature probes placed on the exterior surface would have interfered with the boundary layer. Therefore, it appeared that the only practical method of measuring the wire temperature was to calibrate and use the test wire as a resistance thermometer. Resistance thermometers have been widely used, and are recognized as one of the most accurate temperature measuring instruments available. A popular metal for resistance thermometers, platinum was selected for the test wire. Due to its extensive use in temperature measurement, the properties of platinum have been well established. Among the characteristics of platinum which make it useful in this application are its chemical inertness, and its relatively high electrical resistivity and temperature coefficient of resistivity. The purity of the platinum wire used in this test was unknown; consequently more extensive calibration testing was performed than would have otherwise been necessary.

The test wire used in this experiment was 0.01594 inches in diameter (26 gauge B & S), and 2.59 inches long across the test section. The test wire arrangement is illustrated in Figure 1, p. 8. The test section of the wire was located between the two 34 gauge B & S platinum potential taps. Potential taps of platinum were used to eliminate parasitic thermal emf's. The two potential taps were attached to the test wire by looping one end of the potential tap around the test wire, and then twisting that end of the potential tap around itself. In order to assure a good electrical and mechanical connection, the taps were spot welded to the test wire with a Baldwin Lima Hamilton model VTW 34 welder. The lower end of the wire, the part just below the lower potential tap, was run through the longitudinal axis of a conical piece of plexiglas and held fast to the plexiglas with a solvent resistant cement. The plexiglas cone was positioned with its nose pointing upward. Its details are shown in Figure 2, p. 9. The purpose of the plexiglas was to prevent the boundary layer's starting below the test section. A 0.75 lb. weight was attached to the base of the conical plexiglas to keep the wire straight and vertical.

For temperature calibration the test wire was suspended vertically in a 1000 ml pyrex beaker. The beaker was initially used for the ice bath, and subsequently placed on an electric stove to provide a hot water bath. During the actual tests a 10 gallon, rectangular, glass walled tank was used to hold the various fluids.

A twelve volt storage battery was used as the power supply. Figure 3, p. 10 shows the wiring diagram for the test setup. The current was regulated with three 12.5 ohm rheostats wired in parallel, and its value was determined by measuring the drop across a 0.10005 ohm Leeds and Northrup model 4221 standard resistor. Two Leeds and Northrup model 8686 Precision Millivolt Potentiometers were used to measure the voltages. It was necessary to use a 10:1 voltage divider to reduce the voltage drops which were to be measured to a value in the potentiometer range.

A 0-1000 range millivoltmeter was placed across the standard resistor to make it possible for the operator to adjust to an approximate current setting without having to continually balance the potentiometer. A single pole, single throw switch which was in series with the voltmeter was opened before any readings were taken with the potentiometers.

Two copper-constantan thermocouples were used with an ice bath reference junction to measure the ambient fluid temperature. The thermocouples were calibrated at the steam point.

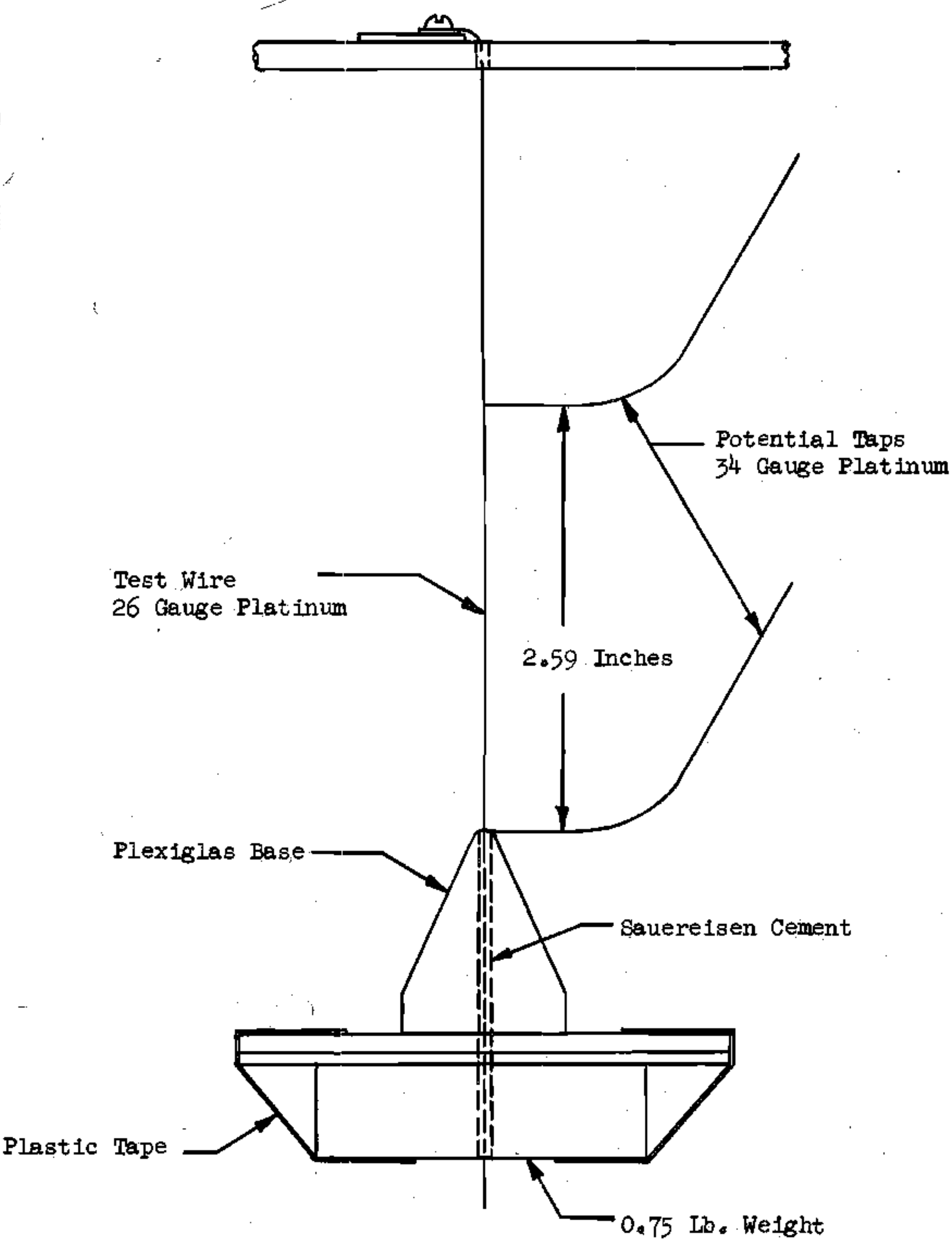

Figure 1. Test Wire Arrangement.

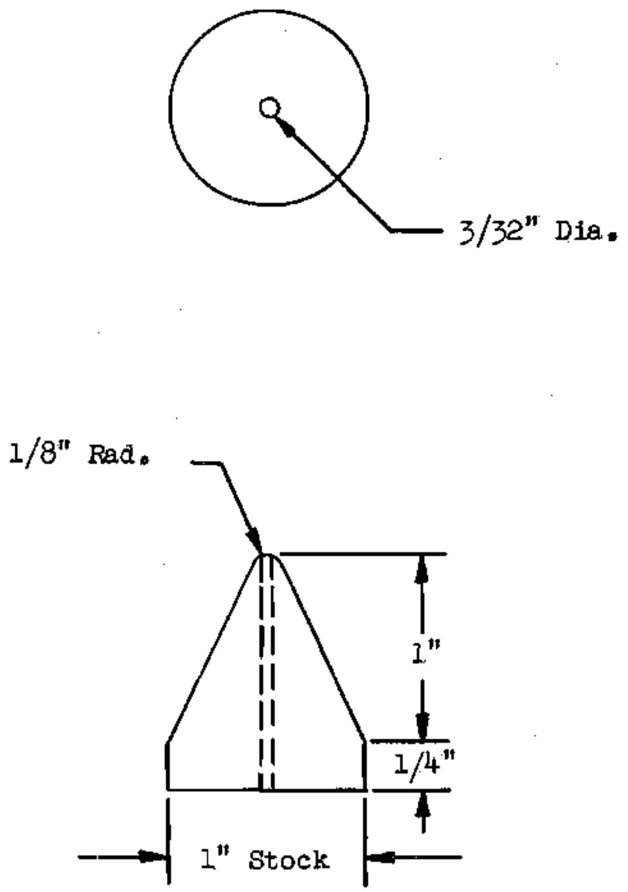

Figure 2. Details of Plexiglas Base.

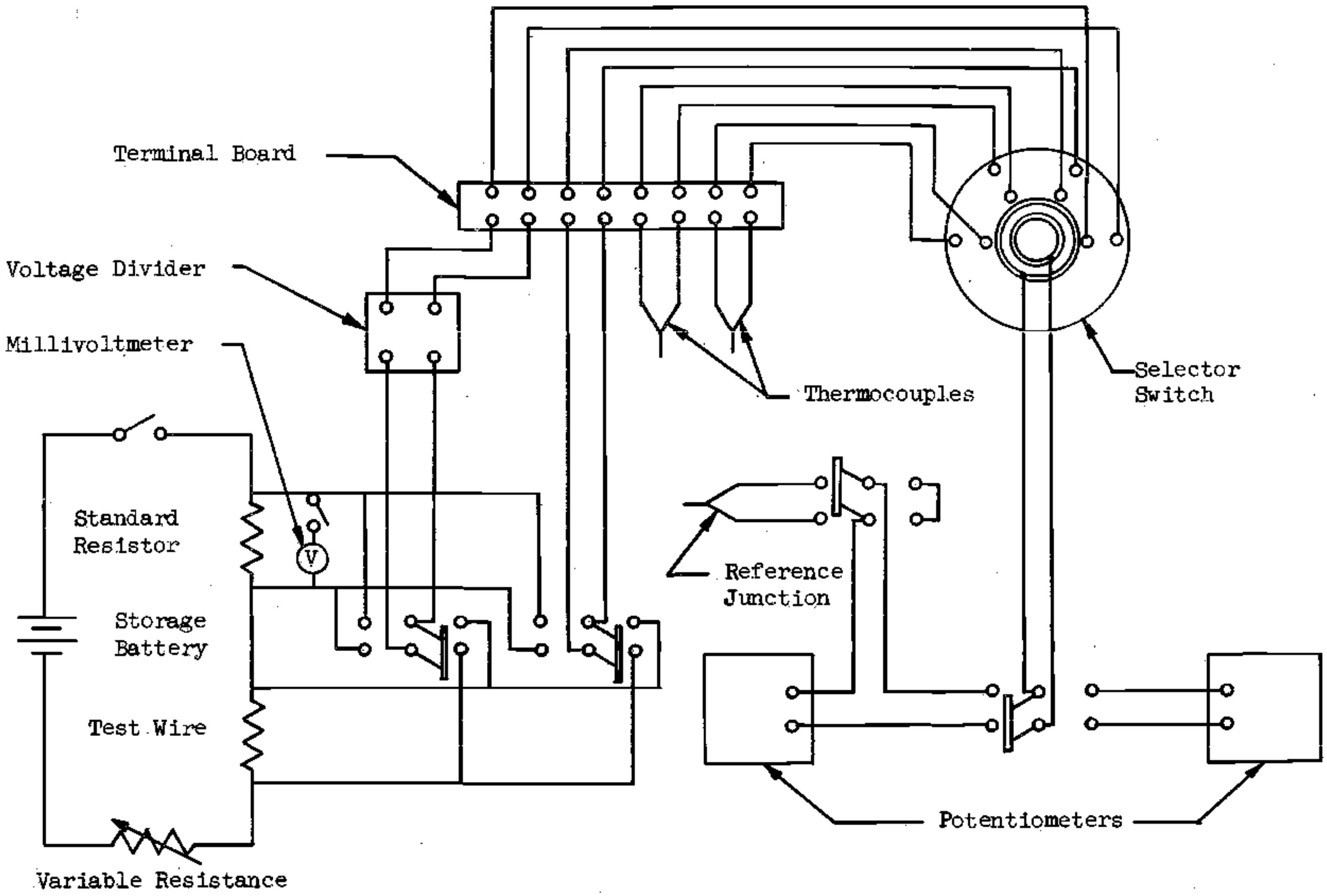

Figure 3. Schematic Diagram of Electrical System.

CHAPTER III

PROCEDURE

Before any data could be taken, it was necessary to calibrate the test wire as a resistance thermometer. Resistance thermometers are usually calibrated by measuring the resistance at three established reference points: the ice point, steam point and sulfur point. Since most of the testing was to be over a rather narrow range of temperatures, calibration at the sulfur point was omitted. Instead, the wire resistance was measured at the ice point, and at several temperatures between the ice point and the steam point. Before beginning the calibration procedure, the platinum wire was annealed at red heat in air for one hour by passing a direct current through it.

For the ice point measurement, the test wire assembly was immersed in a 1000 ml pyrex beaker filled with melting crushed ice and water. A small direct current, around 140 milliamperes, was run through the test wire while the voltage drops across the standard resistor and across the test wire were measured. The resistance was then easily calculated from Ohm's Law, $R = E/I$. After a number of readings had been taken at the ice point, the beaker was refilled with water and placed on an electric stove. Resistance measurements were then made with the water bath at room temperature and at temperatures up to 200° F. A small, electrically powered stirrer was inserted in the water to maintain uniform temperature throughout the fluid. The water temperature was measured with two copper - constantan thermocouples. Following the resistance measurements, the value of the temperature coefficient of resistivity, a, was computed from the relation

$$R = R_o(1 + at_w)$$

and the average value was found to be 0.003820° C^{-1} compared to the value given for fully annealed, C. P. platinum of 0.003926 C^{-1}. It is believed that this discrepancy was due, primarily, to impurities in the platinum test wire.

After the calibration was completed, the test wire was vertically suspended in a ten-gallon, glass walled tank filled with distilled water. The wire was positioned such that the top of the test section was approximately five inches below the free surface of the water. To prevent disturbance of the free surface, the top of the tank was fitted with plywood covers. To eliminate, as much as possible, any extraneous motion of the fluid, the tank was placed on a table which was located away from the other test equipment.

A series of runs was started by closing the main switch which energized the circuit. The current was regulated by adjusting the rheostats. Initial settings were for the lower power inputs. The current was increased in regular jumps of approximately one-half ampere. A millivoltmeter which was placed across the standard resistor allowed the operator to make a rough setting before balancing the potentiometers. A switch in series with the millivoltmeter was opened, once the desired current was obtained, to eliminate any error caused by the small current drawn by the meter circuit. For every run, readings were taken of the drop across the test wire and the standard resistor, and the emf's generated by the two thermocouples used to measure the ambient fluid temperature. Two potentiometers were used: one to measure the test wire voltage, and the other to measure the standard resistor voltage and the thermocouples' emf's. By using two potentiometers, it was possible to measure the test wire and standard resistor voltages almost simultaneously. Both potentiometers were standardized prior to each run.

The same procedure, as outlined above, was used for the tests in air and in oil.

CHAPTER IV

THEORY

Hama, Recesso, and Christiaens presented their solution for a Prandtl number of 0.72 in the form of a table which gave the value of ξ for several values of the dimensionless local heat transfer coefficient $1/\alpha$. From the tabulated values it was possible to obtain solutions for other Prandtl numbers. As can be seen from equation (1) the left band side is function of α only, and

$$F(\alpha) = \frac{1}{32\ Pr}\,\xi^4 = \left[\frac{1}{32\ Pr}\,\xi^4\right]_{air} \tag{2}$$

$$= \left[\frac{1}{32\ Pr}\,\xi^4\right]_{water} = \left[\frac{1}{32\ Pr}\,\xi^4\right]_{oil}.$$

Therefore

$$\frac{\xi_{water}}{\xi_{air}} = \left[\frac{Pr_{water}}{Pr_{air}}\right]^{\frac{1}{4}} \tag{3}$$

$$\frac{\xi_{oil}}{\xi_{air}} = \left[\frac{Pr_{oil}}{Pr_{air}}\right]^{\frac{1}{4}}. \tag{4}$$

Using the above relations, it was possible to convert the existing solution for air ($Pr = 0.72$) into solutions for water and for oil by multiplying the tabulated values of ξ by the corresponding Prandtl number ratio to the one-fourth power.

Average (overall) values of the dimensionless heat transfer coefficient were obtained from the usual definition of the average value:

$$\left(\frac{1}{\alpha}\right)_{avg} = \frac{1}{L}\int_o^L \frac{1}{\alpha}\,dX \ .$$

The integration was performed numerically by the trapezoidal rule. Values of the average Nusselt number for various values of ξ were calculated for air ($Pr = 0.72$), water ($Pr = 4.52$), and oil ($Pr = 162$). The Prandtl numbers in parentheses are the arithmetic average values of all the experimental runs in air, water, and oil respectively.

The expressions used for the average Nusselt numbers for the flat plate for air and for water were those given by Ostrach:

$$Nu_{L\ fp} = 0.6728\left[\frac{Gr_L}{4}\right]^{\frac{1}{4}} \quad \text{for } Pr = 0.72 \ , \tag{5}$$

and

$$Nu_{L\ fp} = 1.1456\left[\frac{Gr_L}{4}\right]^{\frac{1}{4}} \quad \text{for } Pr = 4.52 \ . \tag{6}$$

For oil, a correlation reported by McAdams (6) and verified by the experimental work of Lorenz (7) was used. The expression was

$$Nu_{L\ fp} = 0.7749\ Pr^{\frac{1}{4}}\left[\frac{Gr_L}{4}\right]^{\frac{1}{4}}$$

$$= 2.766\left[\frac{Gr_L}{4}\right]^{\frac{1}{4}} \quad \text{for } Pr = 162 \ . \tag{7}$$

CHAPTER V

DISCUSSION OF RESULTS

The experimental results are compared with the analytical solution of Hama, Recesso, and Christiaens in Figures 4, 5, and 6, and with the solution of LeFevre and Ede in Figures 7, 8, and 9 beginning on p. 19. The arithmetic mean of the percentage deviation of the data from the solution of Hama, Recesso, and Christiaens was 6.23, 14.3 and 3.64 for the water, oil, and air respectively. And the mean percentage deviation from the solution of Le Fevre and Ede was 8.21, 11.1 and 8.15 for the water, oil, and air respectively. It should be noted that the curves which represent the analytical solutions are for a value of the Prandtl number obtained by averaging the values for each of the fluids. For example, the curve in Figure 5 represents the solution for a Prandtl number of 162, which was the arithmetic mean value for the five runs that were made during the oil experiment; however, the data points for the oil represent Prandtl numbers ranging from 96.4 at a ξ of 25 to 242 at a ξ of 66.2. Another factor which results in some deviation of the data from the analytical solutions is that the actual physical setup did not correspond exactly to the mathematical models used in the theory. The test wire, very likely, did not have a perfectly uniform temperature; the measured value was only an average. Some heat was lost by conduction through the potential taps and current leads, and by radiation. These losses, although relatively small, could only be approximately accounted for. Additionally, there was the problem of variable fluid properties. For the water and oil, the properties were evaluated at the arithmetic mean value of the wire temperature and the ambient fluid temperature. This could be especially important with the oil because its viscosity is a strong function of temperature. For the air, the properties, with the exception of the expansion coefficient β which was evaluated at t_∞, were evaluated at the reference temperature

$$t^* = t_w - 0.38(t_w - t_\infty) \tag{8}$$

as recommended by Sparrow (8). Also, the experimental error (see error analysis in Appendix B, p. 35) accounts for some of the disagreement. As expected, the greatest scatter in the data occurred at the low power inputs where small absolute errors give rise to relatively large percentage errors, especially in the temperature difference $(t_w - t_\infty)$. The low power inputs correspond to the high values of ξ and the low values of $\frac{D}{L}(Gr_L Pr)^{\frac{1}{4}}$.

It is interesting to note in Figures 4, 5, and 6 that the curve for water falls under the one for air, and that the curve for oil is lower than the one for water. This indicates that the curvature effect becomes less significant as the Prandtl number is increased. Some insight as to why this occurs may be gained by examining the results of Ostrach for the flat plate. For a given value of ξ, say ξ_1,

$$\xi_1 = \frac{2^{\frac{3}{2}}}{Gr_L^{\frac{1}{4}}} \frac{L}{r_o} .$$

Multiplying both sides by the thermal boundary layer thickness δ_t, and rearranging yields

$$\frac{\delta_t}{r_o} = \frac{\xi_1}{2^{\frac{3}{2}}} \; Gr_L^{\frac{1}{4}} \; \frac{\delta_t}{L} \quad .$$

At a distance from the plate equal to δ_t Ostrach's solution yields

$$Gr_L^{\frac{1}{4}} \; \frac{\delta_t}{L} \approx 4.7 \text{ for } Pr = 0.72, \text{ and}$$

$$Gr_L^{\frac{1}{4}} \; \frac{\delta_t}{L} \approx 0.8 \text{ for } Pr = 100.$$

Therefore for $Pr = 0.72$

$$\frac{\delta_t}{r_o} \approx 4.7 \; \frac{\xi_1}{2^{\frac{3}{2}}} \quad ,$$

and for $Pr = 100$

$$\frac{\delta_t}{r_o} \approx 0.8 \; \frac{\xi_1}{2^{\frac{3}{2}}} \quad .$$

This shows that for a given value of ξ and r_o the thermal boundary layer thickness decreases as the Prandtl number increases.

During the tests Gr_L reached a maximum value of 2.01×10^8 (run number 11 in water). Therefore based on a critical Gr_L of 10^9, the value usually given for vertical plane surfaces, the entire series of tests was in the laminar regime. However there is a possibility that the critical Gr_L is not the same for vertical circular cylinders and vertical plane surfaces.

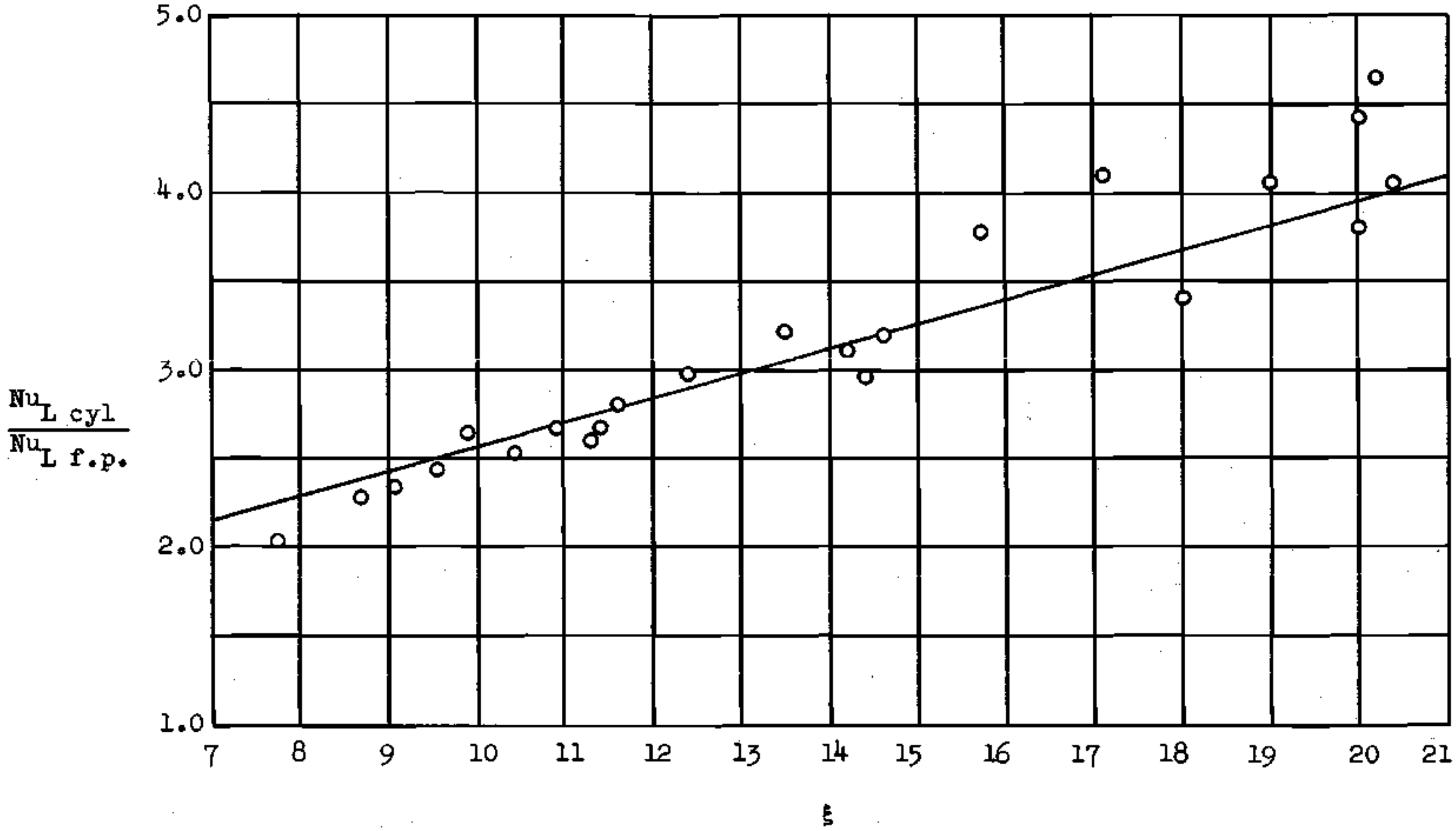

Figure 4. Experimental Data for Water Compared to Solution of Hama, Recesso, and Christiaens for Prandtl Number of 4.52.

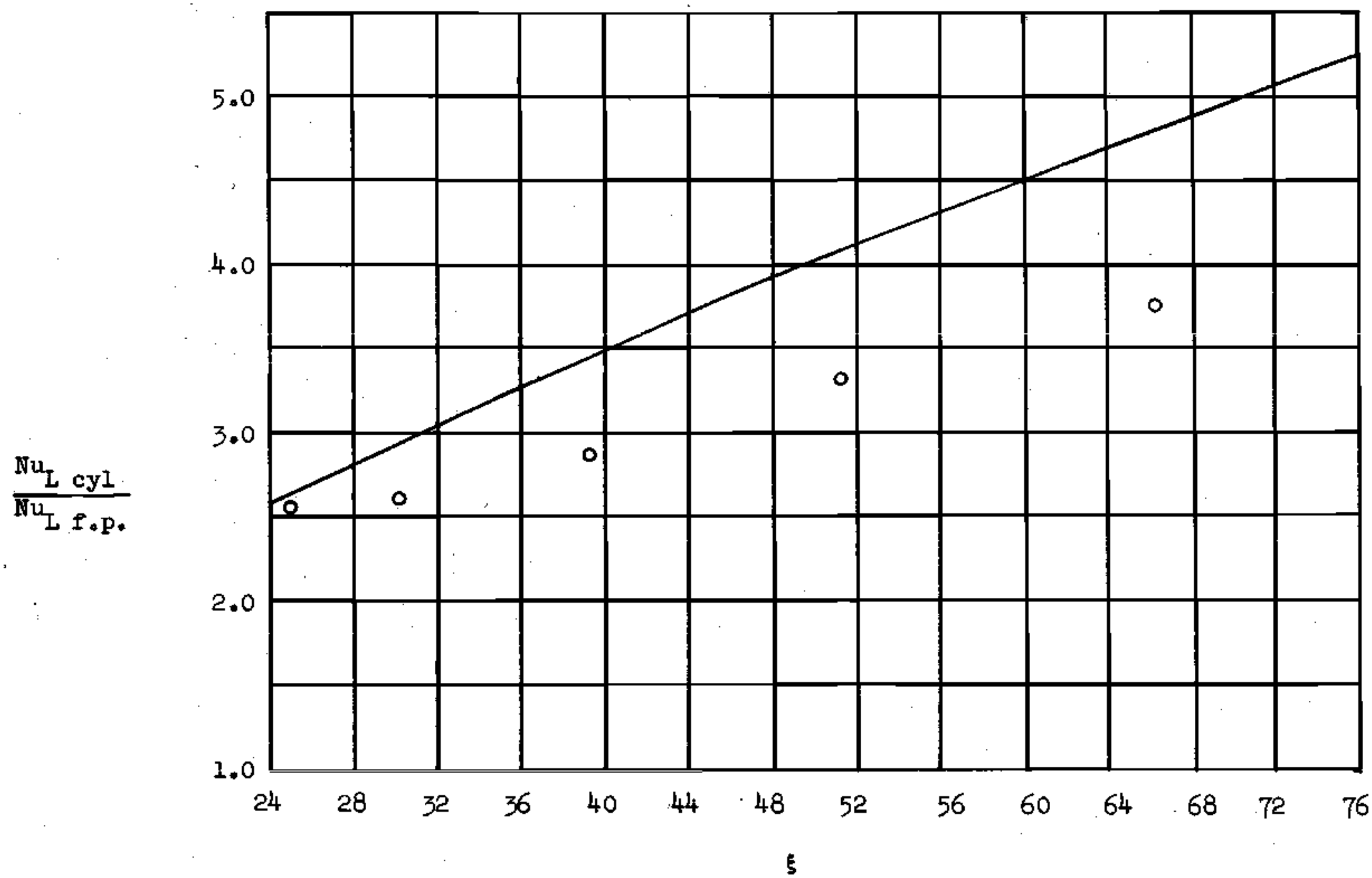

Figure 5. Experimental Data for Oil Compared to Solution of Hama, Recesso, and Christiaens for Prandtl Number of 162.

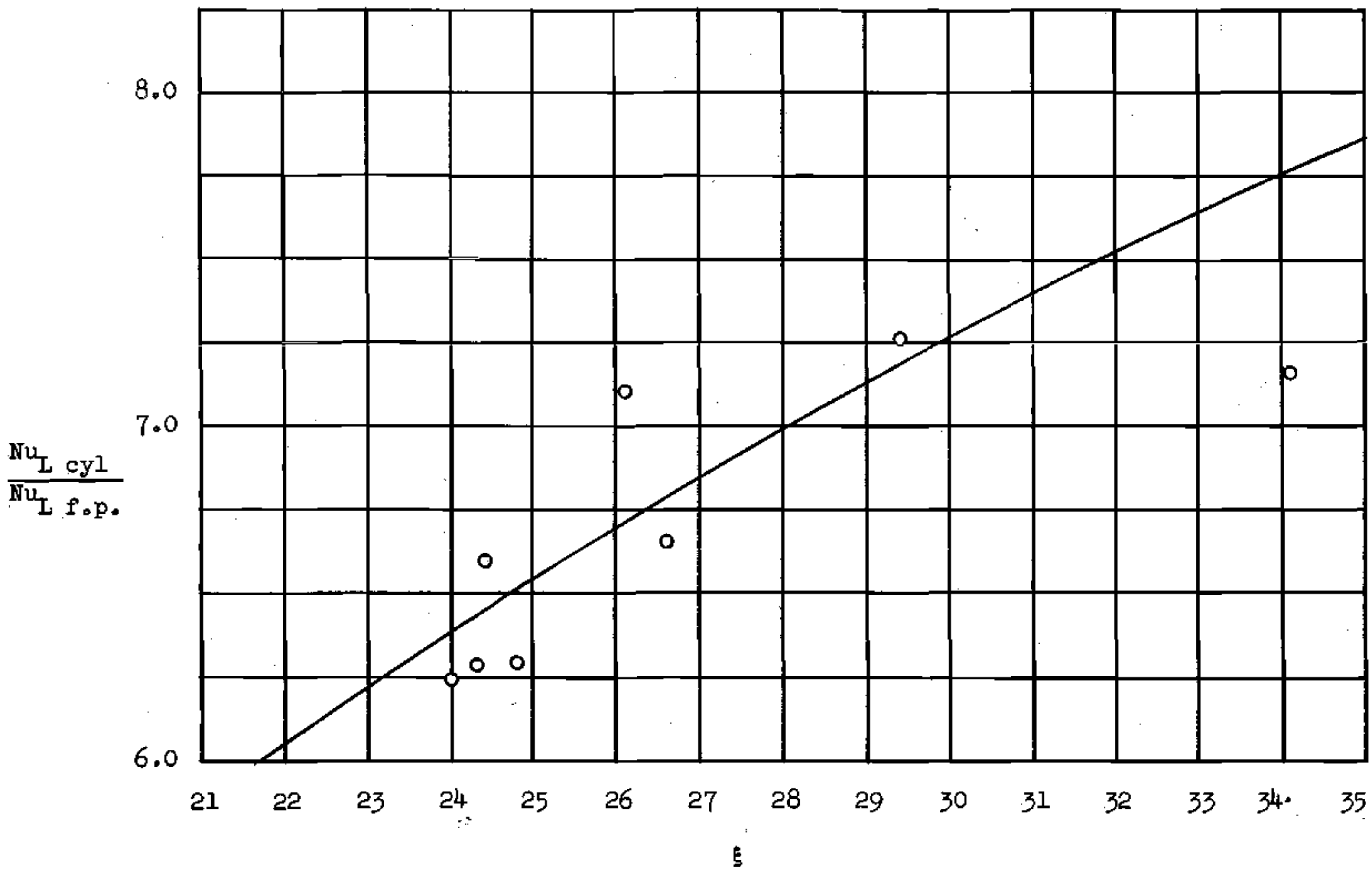

Figure 6. Experimental Data for Air Compared to Solution of Hama, Recesso, and Christiaens for Prandtl Number of 0.72.

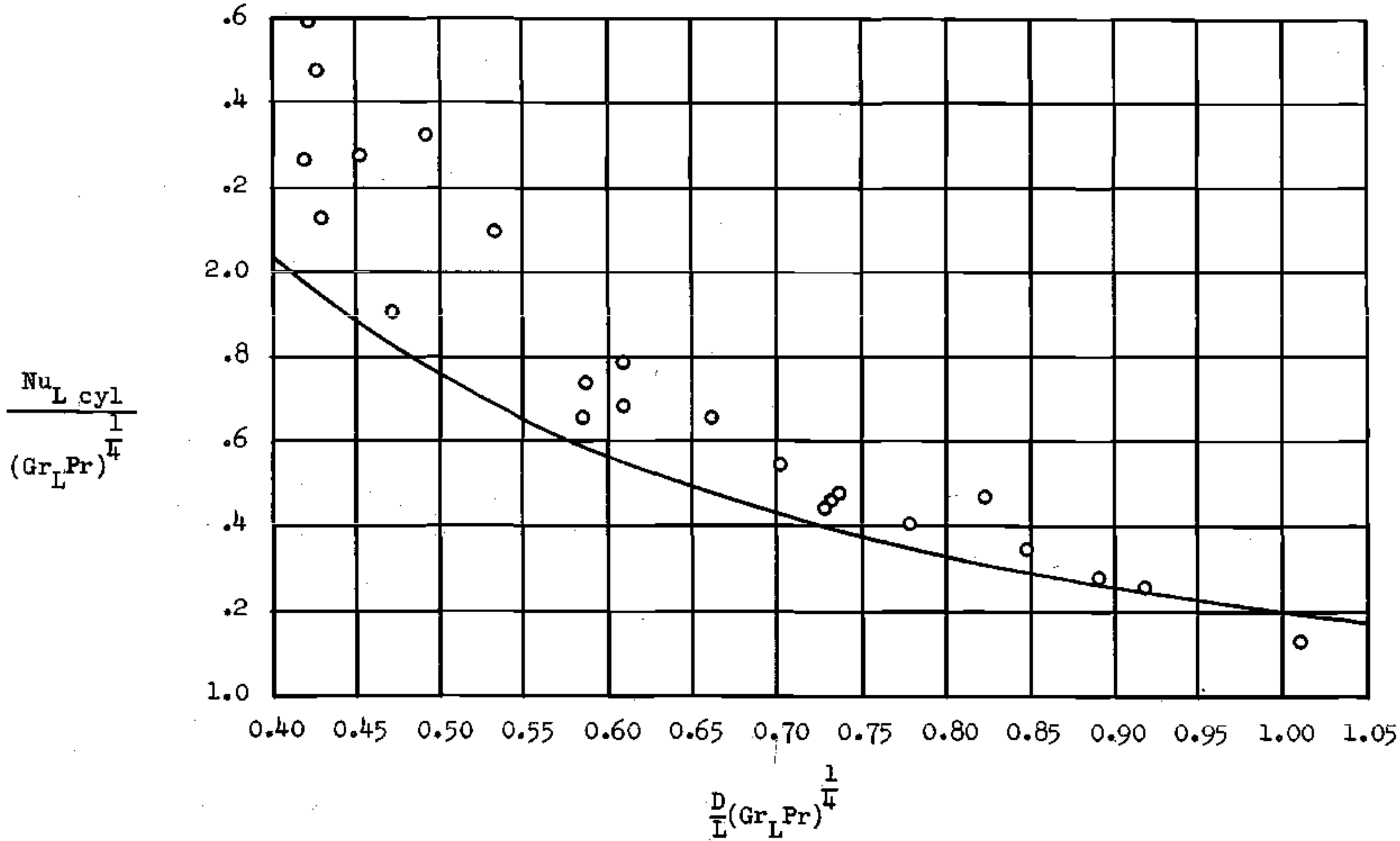

Figure 7. Experimental Data for Water Compared to Solution of LeFevre and Ede for Prandtl Number of 4.52.

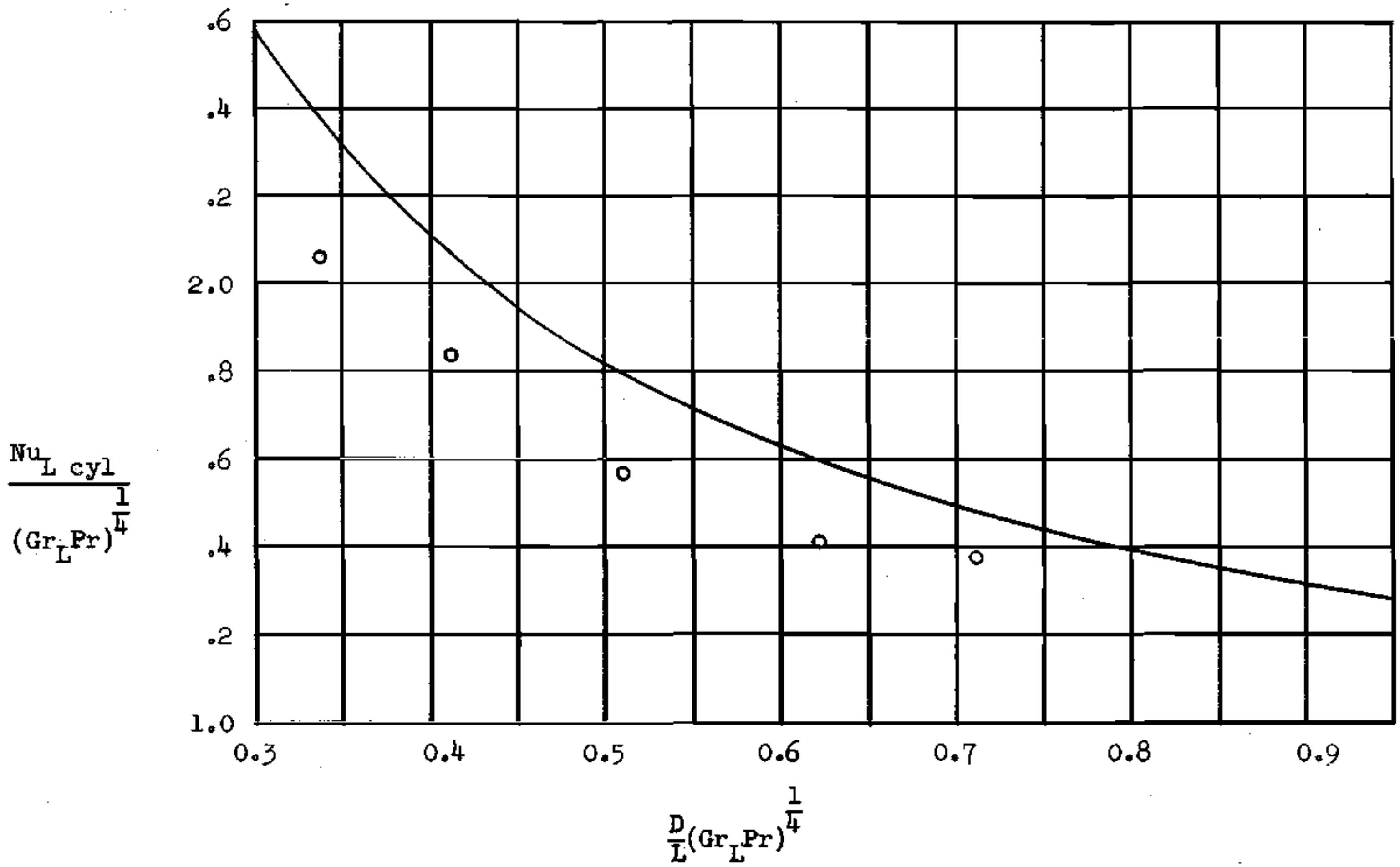

Figure 8. Experimental Data for Oil Compared to Solution of Le Fevre and Ede for Prandtl Number of 162.

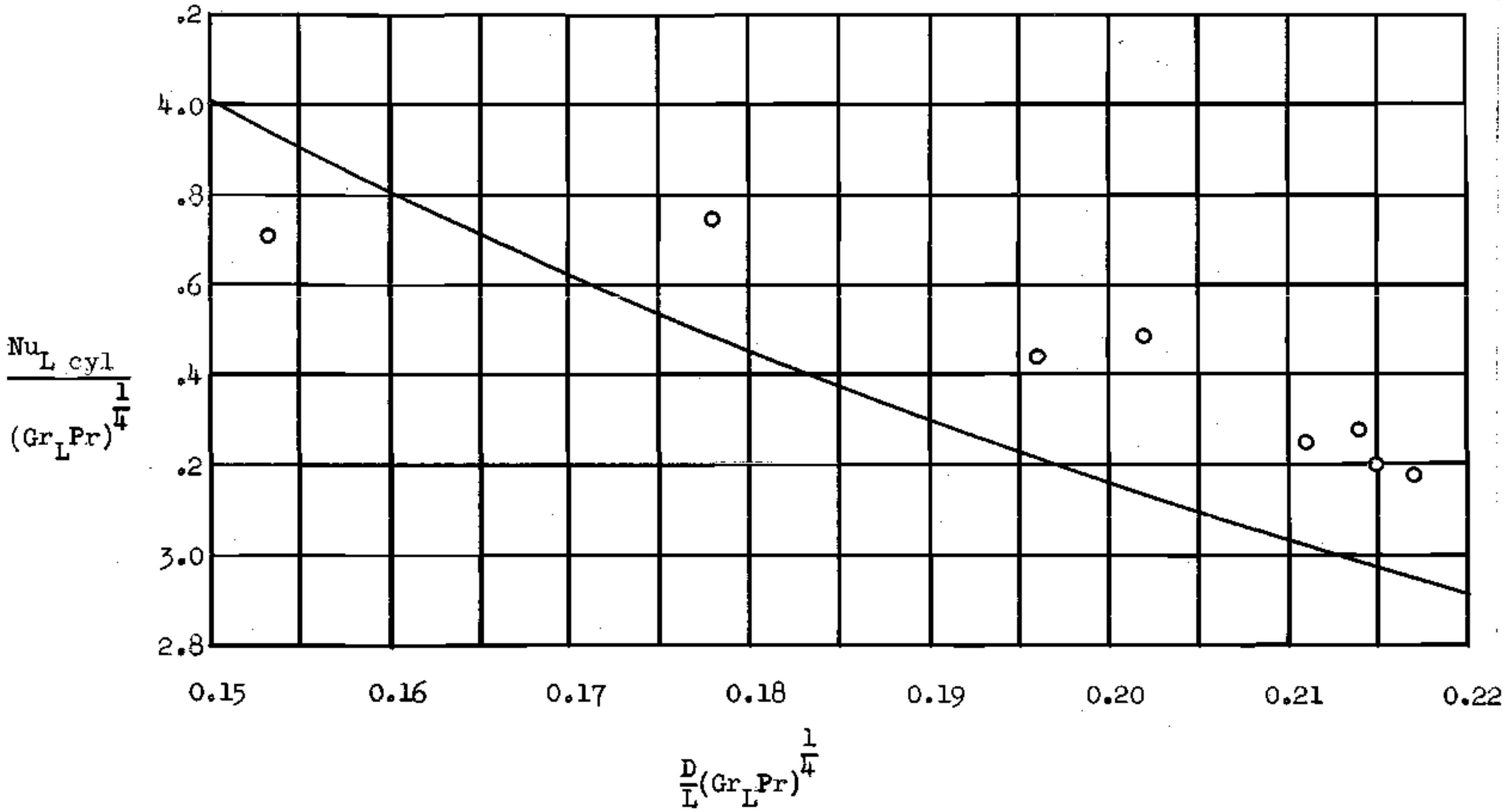

Figure 9. Experimental Data for Air Compared to Solution of Le Fevre and Ede for Prandtl Number of 0.72.

CHAPTER VI

CONCLUSIONS

This experiment has demonstrated that the solutions of Hama, Recesso, and Christiaens and Le Fevre and Ede can be used to predict the average Nusselt number for the problem of laminar free convection heat transfer from a vertical isothermal cylinder suspended in water ($7.72 \leq \xi \leq 20.4$), oil ($25.0 \leq \xi \leq 66.2$), and air ($24.0 \leq \xi \leq 34.1$). It has also been established that the effect of curvature is less pronounced for fluids with high Prandtl numbers.

CHAPTER VII

RECOMMENDATIONS

It is recommended that a higher capacity power supply be used for future work of this kind. This could be done by hooking three or four high capacity twelve volt storage batteries in parallel. It is also recommended that only the highest purity platinum be used whenever the wire is to be used as a resistance thermometer. For further study it is recommended that a series of tests be conducted to obtain data for the range of ξ (for the same or similar fluids) below the range covered by this experiment by using wires of smaller lengths and/or larger diameters, and that a fluid with a very high Prandtl number, such as glycerine, be used in one series of tests.

APPENDICES

APPENDIX A

SAMPLE CALCULATIONS

Calculations in this appendix are for run number four in air. The data and calculated results for this run are given in Table 3, p. 45.

The current I was computed from Ohm's Law.

$$I = \frac{E_{sr}}{R_{sr}} = \frac{0.2526}{0.10005} = 2.525 \text{ amps.}$$

Similarly, the resistance of the test wire,

$$R = \frac{E_{tw}}{I} = \frac{0.2032}{2.525} = 0.0805 \text{ ohms .}$$

The platinum temperature is defined by

$$t_{pt} = \frac{1}{a}\left[\frac{R_{tw}}{R_o} - 1\right] + 32 \qquad (9)$$

For temperatures below 248° F the relation between the resistance of platinum and its temperature is essentially linear, therefore the platinum temperature t_{pt} and t_w can be considered to be equal in this range with negligible error. Therefore the difference between t_{pt} and t_w was neglected for the tests conducted in water and in oil, but for the air tests the difference was accounted for by a form of the Callendar equation given in Reference (9):

$$t_w = t_{pt} + \delta \left[\left(\frac{t_w}{100} \right)^2 - \frac{t_w}{100} \right] \quad (1.8)$$

The constant δ which varies from 1.49 to 1.50 depending on the purity was assumed to be 1.50, the same value as published for C.P. platinum. To eliminate the iteration process required in the above equation, a table (Reference 9) was used which gave the wire temperature t_w for values of the platinum temperature t_{pt} and a value of δ of 1.50. The values of R_o and a were determined by measuring the resistance at 32° F and at several other temperatures up to 200° F, and the average values were found to be 0.0533 ohms and 0.00212° F^{-1} respectively. (See Chapter III for the details of the calibration procedure.) Therefore by equation (9):

$$t_{pt} = \frac{1}{0.00212} \left[\frac{0.0805}{0.0531} - 1 \right] + 32 = 275° \text{ F}$$

Then by using the table in reference (9) the wire temperature

$$t_w = 276° \text{ F}$$

The total heat dissipated by the test wire is given by

$$Q = E_{tw} I \text{ (Watts) x } 3.412 \frac{\text{Btu}}{\text{Watt-hr}}$$

$$= (0.2032)(2.525)(3.412) = 1.751 \frac{\text{Btu}}{\text{hr}} .$$

The heat lost by radiation was computed from

$$Q_{rad} = \sigma \epsilon A \left(T_w^4 - T_\infty^4 \right)$$

where

$$\sigma = 0.1714 \times 10^{-8} \frac{\text{Btu}}{\text{hr} - \text{ft}^2 - (°\text{R})^4}$$

ϵ = 0.051 (Taken from Reference 10 at t_w = 276.3 F)

$$A = \lambda DL = \frac{\lambda(0.01594)(2.59)}{144} = 9.02 \times 10^{-4} \text{ ft}^2 .$$

Then

$$Q_{rad} = (0.1714)(10)^{-8}(0.051)(9.02)(10)^{-4}\left[(736)^4 - (550)^4\right]$$

$$= 0.0161 \frac{\text{Btu}}{\text{hr}} .$$

The heat lost by radiation from the wire for the tests in water and in oil was neglected since it was extremely small: less than 0.02 per cent for the water tests, and less than 0.11 per cent for the oil tests. For all tests the conduction loss through the current leads was assumed negligible, because the axial temperature gradient at the ends of the test section was small due to the fact that heat was generated in the platinum wire extending from the ends of the test section at approximately the same rate as in the test section itself. However the conduction loss through the potential taps was not negligible, and was evaluated by assuming the potential taps to be infinite horizontal fins of constant circular cross section. From Kreith (11) the solution for the infinite fin is

$$Q_{fin} = \sqrt{\bar{h}PKA_c} \quad (t_w - t_\infty)$$

where

$\bar{h}$ = average heat transfer coefficient for the fin.

P = perimeter of the fin.

K = thermal conductivity of the fin.

A_c = cross sectional area of the fin.

The average heat transfer coefficient $\bar{h}$ for the outside surface of the fin was calculated by obtaining the average Nusselt number Nu_D from Reference (12) at a Grashof number Gr_D which was evaluated by assuming a uniform temperature difference equal to $(t_w - t_\infty)$. Then from Reference (12) at $Gr_D = 0.0273$ and $Pr = 0.72$ the mean Nusselt number based on the diameter was found to be 0.713. Then

$$\bar{h} = Nu_D \frac{K}{D} = \frac{(0.713)(0.0175)(12)}{0.0063} = 23.8 \frac{\text{Btu}}{\text{hr-ft}^2\text{-°F}}$$

Brown and Marco (13) report the value of k for platinum as 41.0 Btu/hr ft °F. Then the heat lost through one potential tap is

$$Q_{fin} = \sqrt{(23.8)\lambda\left(\frac{0.0063}{12}\right)(41.9)\left(\frac{\lambda}{4}\right)\left(\frac{0.0063}{12}\right)^2}(276-90) = 0.1115 \frac{\text{Btu}}{\text{hr}}.$$

The total heat lost by conduction through the two potential taps is

$$Q_{cond} = 2(0.1115) = 0.223 \frac{\text{Btu}}{\text{hr}} .$$

The preceding analysis gives a value for the heat conducted through the potential taps which is probably higher than the actual case. Even so, in the entire series of tests the value of Q_{cond} only amounted to a maximum of fifteen per cent of the total heat dissipated Q.

The heat transfer by free convection from the test wire is

$$Q_{conv} = Q - Q_{rad} - Q_{cond}$$

$$= 1.751 - 0.016 - 0.223 = 1.512 \frac{Btu}{hr} .$$

The heat transfer coefficient is

$$h = \frac{Q}{A(t_w - t_\infty)} = \frac{1.512}{(9.020)(10)^{-4}(276 - 90)} = 9.01 \frac{Btu}{hr\text{-}ft^2\text{-}°F} .$$

The properties of air, with the exception of the expansion coefficient β which was evaluated at t_∞, were evaluated at the reference temperature t^* given by equation (8). (The fluid properties of water and oil were evaluated at the arithmetic mean value of t_w and t_∞.) The properties of air and water were taken from Table A - 3 in Reference 4, and the properties of oil were taken from Table 4 in Appendix C, p. 47. The reference temperature t^* was

$$t^* = t_w - 0.38 (t_w - t_\infty)$$

$$= 276 - 0.38 (276 - 90) = 205° \text{ F}$$

The properties of air were then found to be

$$\nu = 0.242 \times 10^{-3} \frac{ft^2}{sec} \qquad K = 0.0175 \frac{Btu}{hr\text{-}ft\text{-}°F}$$

$$Pr = 0.72 \qquad \beta = 1.83 \times 10^{-3} (°F)^{-1}$$

Then the Grashof number based on the length was

$$Gr_L = \frac{g\beta}{\nu^2} L^3 (t_w - t_\infty)$$

$$= \frac{(32.2)(1.83)(10)^{-3} \left(\frac{2.59}{12}\right)^3 (276.3 - 90.0)}{(0.242)^2 (10)^{-6}} = 1.90 \times 10^6 .$$

The average Nusselt number was

$$Nu_{L\ cyl} = \frac{hL}{K} = \frac{(9.01)(2.59)}{(0.0175)(12)} = 111.1 .$$

The average Nusselt number for the vertical flat plate was computed from equation (3).

$$Nu_{L\ fp} = 0.6728 \left[\frac{Gr_L}{4}\right]^{\frac{1}{4}} = 0.6728 \quad \frac{(1.90)(10)^6}{4}^{\frac{1}{4}} = 17.65$$

Then the ratio of the average Nusselt numbers was

$$\frac{Nu_{L\ cyl}}{Nu_{L\ fp}} = \frac{111}{17.65} = 6.29$$

The X-parameter ξ was

$$\xi = \frac{2^{\frac{3}{2}}}{(Gr_L)^{\frac{1}{4}}} \frac{L}{r_o} = \frac{2^{\frac{3}{2}}}{(1.90 \times 10^6)^{\frac{1}{4}}} \quad \frac{(2.59)(2)}{(0.01594)} = 24.8 .$$

The dependent variable in the solution of Le Fevre and Ede was

$$\frac{Nu_{L\ cyl}}{(Gr_L Pr)^{\frac{1}{4}}} = \frac{111}{(1.90 \times 10^6 \times 0.72)^{\frac{1}{4}}} = 3.25$$

and the independent variable was

$$\frac{D}{L}(Gr_L Pr)^{\frac{1}{4}} = \frac{0.01594}{2.59}(1.90 \times 10^6 \times 0.72)^{\frac{1}{4}} = 0.211 .$$

APPENDIX B

ERROR ANALYSIS

In this analysis an estimate is made of the maximum error in the experimentally determined values of the average Nusselt number, $Nu_{L\ cyl}$. The error in the final results is determined largely by the error in measuring the temperature difference $(t_w - t_\infty)$. Therefore the runs at the maximum and minimum values of $(t_w - t_\infty)$ are considered.

Possible Errors

Errors could have occurred in measuring the quantities: wire diameter, wire length, voltage divider ratio, test wire and standard resistor voltages, resistance of the standard resistor, and the temperature of the test wire and the ambient fluid. Errors in Q_{rad} and Q_{cond} result in negligible errors in the final results. This is due to the fact that Q_{rad} and Q_{cond} themselves are a small percentage of the total heat dissipated. It was assumed that negligible error was introduced in determining the fluid properties.

Wire Diameter

The nominal diameter for 26 gauge B & S wire is given as 0.01594 in. The wire diameter was measured with a Bausch and Lomb model DR 22 optical gauge which had an accuracy reported by the manufacturer to be ±0.00005 in. Readings were taken at nine different points along the wire's length, and the average value was 0.01594 in. with a maximum deviation due to non-uniformity of 0.00004 in. Therefore the maximum error in the wire diameter was

$$\frac{0.00005 + 0.00004}{0.01594} (100) = 0.565 \text{ per cent.}$$

Wire Length

Dividers were used to measure the wire length with an accuracy of ±1/64 in. The length was 2-19/32 in. The maximum error in the wire length was

$$\frac{\frac{1}{64}}{\frac{83}{32}} (100) = 0.603 \text{ per cent.}$$

Voltage Divider

The ratio was measured with a Leeds and Northrup Portable Wheatstone Bridge and found to be 9.98 : 1 ± 0.100 per cent.

Voltages

All voltages were measured with Leeds and Northrup model 8686 Precision Millivolt Potentiometers. The accuracy specified by the manufacturer was ± 0.05 per cent of the reading plus 3.0 μv. When the voltage divider was used, the accuracy of the readings was (neglecting the 3.0 μv.)

0.100 per cent + 0.05 per cent = ± 0.150 per cent.

Standard Resistor

The standard resistor was a Leeds and Northrup model 4221. It was checked in the School of Electrical Engineering at Georgia Institute of Technology on a Kelvin Bridge at 25° C, and found to be 0.10005 ohms accurate within ± 0.100 per cent. The change in resistance due to temperature change was considered negligible.

Temperatures

Based on the calibration results, the accuracy of the temperature of the test wire was estimated to be ± 1.0° F. The thermocouples used to measure the ambient fluid temperature were calibrated at the steam point and found to be accurate to ± 1.0° F. The temperature difference $(t_w - t_\infty)$ was assumed accurate to ± 1.5° F. This assumption was made, because prior to heating the test wire t_w and t_∞ agreed within 1.5° F.

Case of Low Temperature Difference

The following is for run number 22 in water. Data and calculated results for this run are given in Table 1, p. 40.

$$Nu_{L\ cyl} = \frac{(3.41)E_{tw}\ E_{sr}}{\lambda DK\ (t_w - t_\infty)\ R_{sr}}$$

$$Nu'_{L\ cyl} = E'_{tw} + E'_{sr} + D' + (t_w - t_\infty)' + R'_{sr} ,$$

where the primes denote the per cent error in a quantity.

$$E'_{tw} = E'_{sr} = 0.150 \text{ per cent}$$

$$D' = 0.565 \text{ per cent}$$

$$(t_w - t_\infty)' = \frac{1.5}{5.15}(100) = 29.2 \text{ per cent}$$

$$R'_{sr} = 0.100 \text{ per cent.}$$

Thus

$$Nu'_L\ cyl = 0.150 + 0.565 + 29.2 + 0.100 = 30.1 .$$

Estimated maximum error in $Nu_{L\ cyl}$ = $\underline{\underline{30.1}}$ per cent.

Case of High Temperature Difference

The following is for run number 8 in air. Data and calculated results for this run are given in Table 3, p. 45.

$$E'_{tw} = E'_{sr} = 0.150 \text{ per cent}$$

$$D' = 0.565 \text{ per cent}$$

$$(t_w - t_\infty)' = \frac{1.5}{885}(100) = 0.170 \text{ per cent}$$

$$R'_{sr} = 0.100 \text{ per cent}$$

Thus

$$Nu'_{L\ cyl} = 0.150 + 0.565 + 0.170 + 0.100 = 0.985 \text{ per cent.}$$

Estimated maximum error in $Nu_{L\ cyl}$ = $\underline{\underline{0.985}}$ per cent.

APPENDIX C

DATA AND CALCULATED RESULTS

Table 1. Data and Calculated Results for Water

Run No.	1	2	3	4	5	6
E_{tw} mv	208.1	237.5	273.8	302.1	341.7	372.0
E_{sr} mv	343.5	389.9	446.5	489.7	549.0	593.2
I amps	3.444	3.897	4.463	4.894	5.488	5.930
R ohms	0.0606	0.0609	0.0614	0.0617	0.0623	0.0627
t_w °F	98.6	101.5	105.2	108.6	113.3	117.4
t_∞ °F	90.1	90.3	89.0	90.4	90.4	90.5
P watts	0.715	0.925	1.222	1.489	1.885	2.21
h $\frac{BTU}{hr\ ft\ °F}$	301	294	168	288	291	291
$Gr_L \times 10^{-6}$	8.44	11.8	17.7	21.4	30.0	39.0
$Gr_L^{\frac{1}{4}}$	53.9	58.6	64.9	68.1	74.0	79.1
Pr	4.87	4.77	4.70	4.55	4.46	4.38
$Nu_{L\ cyl}$	186	182	166	177	178	178
$Nu_{L\ fp}$	45.6	48.2	53.2	55.3	59.7	63.6
$\frac{Nu_{L\ cyl}}{Nu_{L\ fp}}$	4.10	3.78	3.11	3.21	2.99	2.81
ξ	17.1	15.7	14.2	13.5	12.4	11.6
$\frac{Nu_{L\ cyl}}{(Gr_L Pr)^{\frac{1}{4}}}$	2.33	2.10	1.74	1.79	1.66	1.55
$\frac{D}{L}(Gr_L Pr)^{\frac{1}{4}}$	0.492	0.532	0.587	0.609	0.661	0.702

(Continued)

Table 1. (Continued) Data and Calculated Results for Water

Run No.	7	8	9	10	11	12
E_{tw} mv	406.1	433.2	506.2	571.9	655.2	148.8
E_{sr} mv	642.3	680.8	784.4	870.5	969.7	248.8
I amps	6.420	6.805	7.840	8.701	9.692	2.487
R ohms	0.0633	0.0637	0.0646	0.0657	0.0676	0.0598
t_w °F	122.0	125.6	133.7	144.0	160.6	91.5
t_∞ °F	90.6	89.7	87.5	87.5	87.7	86.0
P watts	2.61	2.95	3.97	4.98	6.35	0.370
h $\frac{BTU}{hr\ ft\ °F}$	295	292	305	313	310	237
$Gr_L \times 10^{-6}$	50.3	60.7	86.8	125	201	4.54
$Gr_L^{\frac{1}{4}}$	84.5	88.3	96.5	106	119	46.1
Pr	4.29	4.25	4.14	3.96	3.66	5.23
$Nu_{L\ cyl}$	180	178	185	189	186	148
$Nu_{L\ fp}$	67.4	70.3	76.3	82.6	91.0	39.1
$\frac{Nu_{L\ cyl}}{Nu_{L\ fp}}$	2.67	2.53	2.44	2.29	2.04	3.80
ξ	10.9	10.4	9.53	8.69	7.72	20.0
$\frac{Nu_{L\ cyl}}{(Gr_L Pr)^{\frac{1}{4}}}$	1.50	1.41	1.35	1.26	1.13	2.13
$\frac{D}{L}(Gr_L Pr)^{\frac{1}{4}}$	0.736	0.779	0.846	0.918	1.01	0.429

(Continued)

Table 1. (Continued) Data and Calculated Results for Water

Run No.	13	14	15	16	17	18
E_{tw} mv	177.3	272.1	405.1	552.3	148.0	175.8
E_{sr} mv	295.4	445.8	644.3	847.6	248.2	294.0
I amps	2.952	4.456	6.440	8.471	2.481	2.938
R ohms	0.0601	0.0611	0.0629	0.0652	0.0596	0.0598
t_w °F	93.7	102.6	118.8	139.2	90.0	91.7
t_∞ °F	85.7	85.7	85.7	85.1	84.7	84.8
P watts	0.523	1.212	2.61	4.68	0.367	0.517
h $\frac{BTU}{hr\ ft\ °F}$	235	255	280	307	248	268
$Gr_L \times 10^{-6}$	6.73	16.8	44.4	107	4.11	5.53
$Gr_L^{\frac{1}{4}}$	51.0	64.0	81.6	102	45.0	48.5
Pr	5.15	4.88	4.44	4.09	5.33	5.26
$Nu_{L\ cyl}$	146	159	172	187	155	168
$Nu_{L\ fp}$	43.1	53.1	66.0	80.1	38.4	41.3
$\frac{Nu_{L\ cyl}}{Nu_{L\ fp}}$	3.40	2.97	2.60	2.33	4.05	4.06
ξ	18.0	14.4	11.3	9.04	20.4	19.0
$\frac{Nu_{L\ cyl}}{(Gr_L Pr)^{\frac{1}{4}}}$	1.91	1.66	1.45	1.28	2.27	2.28
$\frac{D}{L} (Gr_L Pr)^{\frac{1}{4}}$	0.471	0.585	0.728	0.890	0.420	0.452

(Continued)

Table 1. (Continued) Data and Calculated Results for Water

Run No.	19	20	21	22	23
E_{tw} mv	274.1	406.5	509.4	157.9	157.4
E_{sr} mv	450.3	647.6	794.5	263.8	263.0
I amps	4.501	6.473	7.941	2.636	2.628
R ohms	0.0609	0.0628	0.0642	0.0599	0.0599
t_w °F	101.2	117.9	130.0	92.1	92.1
t_∞ °F	84.9	84.9	85.3	87.0	86.7
P watts	1.234	2.63	4.04	0.416	0.414
h $\frac{BTU}{hr\ ft\ °F}$	269	283	321	288	276
$Gr_L \times 10^{-6}$	15.6	42.4	75.4	4.35	4.48
$Gr_L^{\frac{1}{4}}$	62.9	80.6	93.2	45.6	46.0
Pr	4.94	4.47	4.25	5.16	5.18
$Nu_{L\ cyl}$	167	174	197	179	172
$Nu_{L\ fp}$	52.3	65.1	74.2	38.5	38.9
$\frac{Nu_{L\ cyl}}{Nu_{L\ fp}}$	3.19	2.67	2.65	4.65	4.42
ξ	14.6	11.4	9.87	20.2	20.0
$\frac{Nu_{L\ cyl}}{(Gr_L Pr)^{\frac{1}{4}}}$	1.69	1.46	1.47	2.60	2.48
$\frac{D}{L}(Gr_L Pr)^{\frac{1}{4}}$	0.608	0.731	0.822	0.423	0.427

Table 2. Data and Calculated Results for Oil

Run No.	1	2	3	4	5
E_{tw} mv	124.4	188.2	263.7	363.8	456.3
E_{sr} mv	203.4	297.0	396.2	510.9	605.9
I amps	2.033	2.969	3.960	5.107	6.056
R ohms	0.0612	0.0634	0.0666	0.0712	0.0754
t_w °F	103.8	123.2	151.7	192.9	229.3
t_∞ °F	85.3	85.5	85.3	85.4	85.4
P watts	0.253	0.559	1.044	1.858	2.76
h $\frac{BTU}{hr\ ft^2\ °F}$	44.7	48.4	51.4	56.4	62.8
$Gr_L \times 10^{-4}$	3.71	10.6	29.9	87.2	184
$Gr_L^{\frac{1}{4}}$	13.9	18.0	23.4	30.5	36.8
Pr	242	196	157	120	96.4
$Nu_{L\ cyl}$	113	123	130	143	160
$Nu_{L\ fp}$	30.0	36.9	45.4	55.3	63.1
$\frac{Nu_{L\ cyl}}{Nu_{L\ fp}}$	3.76	3.32	2.87	2.61	2.53
ξ	66.2	51.1	39.3	30.2	25.0
$\frac{Nu_L}{(Gr_L Pr)^{\frac{1}{4}}}$	2.06	1.84	1.57	1.41	1.38
$\frac{D}{L}(Gr_L Pr)^{\frac{1}{4}}$	0.337	0.412	0.510	0.623	0.711

Table 3. Data and Calculated Results for Air

Run No.	1	2	3	4	5
E_{tw} mv	63.17	101.7	142.5	203.2	270.5
E_{sr} mv	100.3	152.4	198.2	252.6	299.8
I amps	1.002	1.524	1.981	2.525	2.996
R ohms	0.0630	0.0668	0.0720	0.0805	0.0903
t_{pt} °F	120.0	153.0	199.3	274.8	361.8
t_w °F	119.3	152.5	199.2	276.3	366.3
t_∞ °F	88.8	89.2	89.5	90.0	91.0
P watts	0.0633	0.1549	0.282	0.513	0.810
h $\frac{BTU}{hr\ ft^2\ °F}$	6.65	7.99	8.40	9.01	9.60
$Gr_L \times 10^{-6}$	0.529	0.965	1.42	1.90	2.06
$Gr_L^{\frac{1}{4}}$	27.0	31.3	34.6	37.1	37.8
Pr	0.72	0.72	0.72	0.72	0.71
$Nu_{L\ cyl}$	92.1	108.0	109.4	111.1	111.6
$Nu_{L\ fp}$	12.84	14.89	16.46	17.65	17.77
$\frac{Nu_{L\ cyl}}{Nu_{L\ fp}}$	7.17	7.26	6.66	6.29	6.28
ξ	34.1	29.4	26.6	24.8	24.3
$\frac{Nu_{L\ cyl}}{(Gr_L Pr)^{\frac{1}{4}}}$	3.71	3.74	3.44	3.25	3.20
$\frac{D}{L}\ (Gr_L Pr)^{\frac{1}{4}}$	0.1529	0.1780	0.1960	0.211	0.215

Table 3. (Continued) Data and Calculated Results for Air

Run No.	6	7	8
E_{tw} mv	347.0	465.7	756.3
E_{sr} mv	344.2	397.0	494.0
I amps	3.440	3.968	4.938
R ohms	0.1009	0.1174	0.1532
t_{pt} °F	455.7	602.1	919.7
t_w °F	467.8	622.4	980.6
t_∞ °F	89.1	91.1	95.7
P watts	1.194	1.848	3.73
h $\frac{BTU}{hr\ ft^2\ °F}$	10.30	11.39	13.57
$Gr_L \times 10^{-6}$	2.15	2.02	1.55
$Gr_L^{\frac{1}{4}}$	38.3	37.7	35.3
Pr	0.71	0.688	0.687
$Nu_{L\ cyl}$	112.3	113.9	114.6
$Nu_{L\ fp}$	18.00	17.26	16.12
$\frac{Nu_{L\ cyl}}{Nu_{L\ fp}}$	6.24	6.60	7.11
ξ	24.0	24.4	26.1
$\frac{Nu_{L\ cyl}}{(Gr_L Pr)^{\frac{1}{4}}}$	3.18	3.28	3.49
$\frac{D}{L}(Gr_L Pr)^{\frac{1}{4}}$	0.217	0.214	0.202

Table 4. Properties of Oil*

Temperature °F	Specific Gravity	$\beta \times 10^4$ $(°R)^{-1}$	$\nu \times 10^4$ ft^2/sec	K Btu/hr ft °F	C_p Btu/lbm °R
80	0.848	3.83	3.32	0.093	0.44
100	0.842	3.86	2.29	0.093	0.46
140	0.829	3.92	1.24	0.092	0.48
180	0.816	3.98	0.764	0.092	0.50
220	0.803	4.05	0.527	0.091	0.51

*The oil used in this test was Ramol 100, a white mineral oil manufactured by Sherwood Refining Division of the Continental Oil Company, Englewood, New Jersey. The properties given in the above table, with the exception of c_p, were determined experimentally in associated tests. The values of c_p were estimated from the specific heat values of similar oils.

APPENDIX D

NOMENCLATURE

A	area of the wire surface
a	platinum temperature coefficient of resistivity
D	test wire diameter
E_{sr}	voltage drop across standard resistor
E_{tw}	voltage drop across test wire
Gr_L	$(g\beta/\nu^2)(t_w - t_\infty)(L)^3$, Grashof number based on wire length.
g	gravitational acceleration
h	free convection heat transfer coefficient
I	test wire current
k	thermal conductivity
L	test wire length
$Nu_{L\ cyl}$	average Nusself number based on length of wire
$Nu_{L\ fp}$	average Nusselt number based on length of flat plate
P	power input to test wire
Pr	Prandtl number
Q	total heat dissipated by test wire
Q_{cond}	conduction heat transfer from test wire through potential taps
Q_{conv}	free convection heat transfer from test wire
Q_{rad}	radiation heat transfer from test wire
R	electrical resistance of test wire
R_o	electrical resistance of test wire at 32° F
R_{sr}	electrical resistance of standard resistor

r_o	radius of test wire
t_w	test wire temperature
t_∞	temperature of surrounding fluid
X	distance from leading edge of cylinder
α	$k(t_w - t_\infty)/r_o Q_{conv}$, reciprocal of dimensionless local heat transfer coefficient
β	temperature coefficient of volume expansion
ϵ	emissivity of test wire surface
ν	kinematic viscosity
ξ	$2^{\frac{3}{2}} (L/r_o)(Gr_L)^{-\frac{1}{4}}$, dimensionless x-parameter
σ	0.1714×10^{-8} Btu/hr ft^2 R^4, Stefan-Boltzmann constant

BIBLIOGRAPHY

LITERATURE CITED

1. H. J. Merk and J. A. Prins, Applied Scientific Research 4A, 22, (1953).

2. S. Ostrach, National Advisory Committee for Aeronautics Technical Note 2635 (1952).

3. E. M. Sparrow and J. L. Gregg, American Society of Mechanical Engineers Transactions 78, 1823 - 1829 (1956).

4. E. J. Le Fevre and A. J. Ede, Ninth International Congress of Applied Mechanics Proceedings, 4, 175 - 183 (1956).

5. F. R. Hama, J. V. Recesso, and J. Christiaens, Journal of the Aerospace Sciences, 26, 335 - 342 (1959).

6. W. H. McAdams, Heat Transmission, 2nd ed., McGraw-Hill Book Co., New York, N. Y. (1942), p. 242.

7. H. H. Lorenz, Zeitschrift für technische Physik 9, 362 - 366 (1934).

8. E. M. Sparrow, Trans. ASME, 80, 879 (1958).

9. G. W. C. Kaye and T. H. Laby, Physical and Chemical Constants, 12th ed. Longmans, Green and Co., London, Eng. (1959), p. 45.

10. W. F. Roeser and H. T. Wensel, Temperature - Its Measurement and Control in Science and Industry, Reinhold Publishing Corp., New York, N. Y. (1941), pp. 1293 - 1326.

11. F. Kreith, Principles of Heat Transfer, International Textbook Co., Scranton, Pa. (1958), p. 47.

12. F. Kreith, op. cit., p. 305.

13. A. I. Brown and S. M. Marco, Introduction to Heat Transfer, 3rd ed., McGraw-Hill Book Co., New York, N. Y. (1958), p. 14.

14. F. Kreith, op. cit., p. 535.